Available online at www.sciencedirect.com
SCIENCE DIRECT
Journal of Sound and Vibration 296 (2006) 277–291
JOURNAL OF SOUND AND VIBRATION
www.elsevier.com/locate/jsvi

In-plane stability analysis of non-uniform cross-sectioned curved beams

Hasan Öztürk[a], İsa Yeşilyurt[b], Mustafa Sabuncu[a,*]

[a]Department of Mechanical Engineering, Faculty of Engineering, Dokuz Eylul University, Bornova, Izmir 35100, Turkey
[b]Department of Mechanical Engineering, Faculty of Engineering, Usak University, Usak 64300, Turkey

Received 23 May 2005; received in revised form 1 March 2006; accepted 3 March 2006
Available online 12 May 2006

Abstract

In this study, in-plane stability analysis of non-uniform cross-sectioned thin curved beams under uniformly distributed dynamic loads is investigated by using the Finite Element Method. The first and second unstable regions are examined for dynamic stability. In-plane vibration and in-plane buckling are also studied. Two different finite element models, representing variations of cross-section, are developed by using simple strain functions in the analysis. The results obtained from this study are compared with the results of other investigators in existing literature for the fundamental natural frequency and critical buckling load. The effects of opening angle, variations of cross-section, static and dynamic load parameters on the stability regions are shown in graphics.

1. Introduction

Research on the dynamic and static stability of curved beams continues to be one of the most interesting subjects in recent years. Especially in turbine blades and bridges, it shows itself as a problem of elastic instability. The dynamic stability of mechanical systems, according to Bolotin's definition [1], represents a specific stability of motion. When Bolotin's approach [1] is examined, three stages, static stability (buckling analysis), vibration analysis and dynamic stability analysis, are seen to be included in the equation of dynamic stability. Therefore these three stages are studied in this paper.

Sabir and Aswell [2] have discussed the natural frequency analysis of circular arches deformed in a plane. The finite elements developed by using different types of shape functions were employed in their analysis. Petyt and Fleischer [3] have studied the free vibration of a curved beam under various boundary conditions. Yıldırım [4] has developed a computer program for the free vibration analysis of arcs. The coupled twist-bending vibrations of complete, incomplete and transversely supported rings have been investigated by Rao [5]. Moshe and Efraim [6] have investigated in-plane vibrations of shear-deformable curved beams. The exact dynamic stiffness matrix for a circular beam was used in this study. Sabuncu [7] has also investigated the vibration analysis of thin curved beams. He used several types of shape functions to develop different curved

*Corresponding author. Tel.: +90 232 3883138/208; fax: +90 232 3887868.
E-mail address: mustafa.sabuncu@deu.edu.tr (M. Sabuncu).

0022-460X/$ - see front matter © 2006 Elsevier Ltd. All rights reserved.
doi:10.1016/j.jsv.2006.03.002

Nomenclature

A	cross-sectional area
A_{Root}	cross-sectional area at root of the beam
b_R	width at the root of the curved beam
b_t	width at the top of the curved beam
E	Young's modulus
I_{Root}	second moment of area of cross-section at root of the beam
I_{xx}	second moment of area of cross-section
k_{cr}	critical buckling load parameter
$\mathbf{k}_e$	elastic stiffness matrix of the elemental finite element
$\mathbf{K}_e$	global elastic stiffness matrix
$\mathbf{k}_g$	geometric stiffness matrix of the elemental finite element
$\mathbf{K}_g$	global geometric stiffness matrix
$\mathbf{M}$	global mass (inertia) matrix
$\mathbf{m}_e$	mass (inertia) matrix of the elemental finite element
$P(t)$	periodic load
P_{cr}	critical buckling load
$\mathbf{q}$	generalized coordinates
R	radius of the curved beam
T	kinetic energy
t_R	thickness at the root of the curved beam
t_t	thickness at the top of the curved beam
U	strain energy
v	circumferential deflection
V	strain energy of the periodic force
w	radial deflection
Ω	disturbing frequency
β	dynamic load parameter
ρ	mass density
ω	natural frequency
θ	opening angle of the curved beam
ϕ	opening angle of the finite element
ψ	rotation of tangent
α	static load parameter
λ	fundamental frequency parameter
ω_1	fundamental frequency of a curved beam

beam finite elements and pointed out the effect of displacement functions on the natural frequencies by comparing the results. In-plane vibration of a tapered curved beam has been studied by Sabuncu and Erim [8]. They presented a finite element model for the vibration analysis of a tapered curved beam. Linear and non-linear variations of cross-sections were considered in their analysis. Chidamparam and Leissa [9] have organized and summarized the extensive published literature on the vibrations of curved bars, beams, rings and arches of arbitrary shape which lie in a plane. They also considered in-plane, out-of-plane and coupled vibration and examined various theories that have been developed to model curved beam vibration problems. In addition, they have studied the free vibrations of circular arches about a prestressed static equilibrium state [10]. Rossi et al. [11], Gutierrez et al. [12] and Rossi [13] have investigated the in-plane vibration of non-circular arcs having non-uniform cross-section with a tip mass. Shear force and rotatory inertia effects were taken into account. They used the finite element approach and the Ritz method in their analysis. Free and forced in-plane vibrations of circular arches with variable cross-sections and various boundary conditions, have been investigated by Tong et al. [14]. Oh et al. [15] have examined free vibration of non-circular arches with non-uniform cross-section. In their study, the differential equations were derived and solved numerically for the parabolic, catenary and elliptic geometries with different boundary conditions. Kawakami et al. [16] have used an approximate method to study the analysis for both the in-plane and out-of-plane free vibration of horizontally curved beams with arbitrary shapes and variable cross-sections. In-plane free vibration analysis of circular arches with varying cross-sections using differential quadrature method (DQM) has been studied by Karami and Malekzadeh [17]. Arches with different types of boundary conditions, including those with elastic constraint against rotation at their ends, were considered in their analysis.

Timoshenko and Gere [18] have examined the buckling analysis of hinged–hinged Bernoulli–Euler curved beams by using the analytical method. Bazant and Cedolin [19] have discussed the buckling analysis of curved beams by using analytical and energy methods. The buckling analysis of a curved beam has been studied by Yoo et al. [20]. They used the Finite Element Method in their analysis. Papangelis and Trahair [21,22] have studied in-plane and lateral buckling of curved beams by using the finite element analysis. Yang et al. [23,24] have examined static stability of curved beams. They employed the non-linear equations of equilibrium for a horizontally curved I-beam and straight-beam approach for the buckling analysis. Natural frequencies and

buckling loads of a simply supported shallow circular arch with sufficiently small depth-to-radius of curvature ratio subjected to initial axial tensile and /or compressive forces have been analyzed by Matsunaga [25]. The DQM has been applied to computation of the eigenvalues of the equations of motion governing the free in-plane vibration included extensibility of the arch axis and the coupled out-of-plane twist-bending vibrations of circular arches by Kang et al. [26]. Pi et al. [27] have investigated the in-plane buckling of circular arches with an arbitrary cross-section and subjected to a radial load uniformly distributed around the arch axis. An energy method was employed to establish both non-linear equilibrium equations and buckling equilibrium equations for shallow arches. Huang et al. [28] have marked on in-plane free vibration and static stability of loaded and shear-deformable circular arches. Chen and Shen [29] have studied vibration and buckling of initially stressed curved beams by using the principle of virtual work.

The dynamic stability of beams under a periodical axial load by using the Finite Element Method and Bolotin's approach, has been studied by Thomas and Abbas [30]. Takahashi et al. [31] have analyzed the dynamic instability of a circular arch subjected to an in-plane sinusoidal varying load by using a multiple-degrees-of-freedom approach, the Galerkin method and the harmonic balance method. Briseghella et al. [32] have investigated the dynamic stability of elastic structures using the Finite Element approach and discussed the damping effects on the dynamic stability. Free vibration and spatial stability of non-symmetric thin-walled curved beams with variable curvatures have been examined by Kim et al. [33].

This paper presents the in-plane static and dynamic stabilities of non-uniform cross-sectioned curved beams subjected to uniformly distributed periodic loading. The equation of motion of a curved beam subjected to a uniformly distributed periodic force brings out Mathieu–Hill type differential equations. In this study, Bolotin's approach is considered and thin curved beams having fixed–fixed boundary conditions are examined by using the Finite Element Method. Two different finite element models, step and continuous, developed are used to represent the linear taper of non-uniform cross-section curved beams. The first and second unstable regions are studied in this paper. The results obtained, on buckling and fundamental frequency, are compared with the results of other investigators in existing literature. The effects of the variation of the cross-section, the opening angle of the arch, static and dynamic load parameters on the stability are examined and the results are given in tables and graphics.

2. Models of curved beams

The boundary conditions and applied loading on a curved beam are shown in Fig. 1. The curved beams examined in this study, have uniform and non-uniform rectangular cross-sections as shown in Fig. 2. The variation of cross-section of the linear tapered curved beam is represented by mathematical expressions as given in Eq. (1). The cross-sections have five different configurations, which for simplicity, are denoted by $C1$, $C2$, $C3$, $C4$ and $C5$. The explanation of these cross-sections is as follows:

$C1$: Uniform ($t_R = t_t$, $b_R = b_t$, Fig. 2a),
$C2$: Unsymmetric tapered with constant width ($t_R \neq t_t$, $b_R = b_t$, Fig. 2b),
$C3$: Double unsymmetric tapered ($t_R \neq t_t$, $b_R \neq b_t$, Fig. 2c),

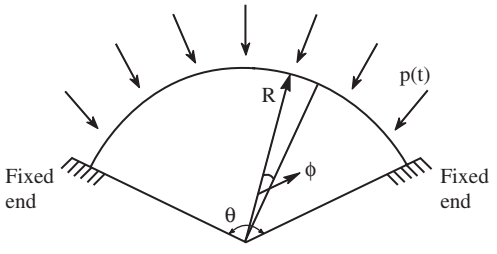

Fig. 1. Curved beam loaded by uniformly distributed periodic force.

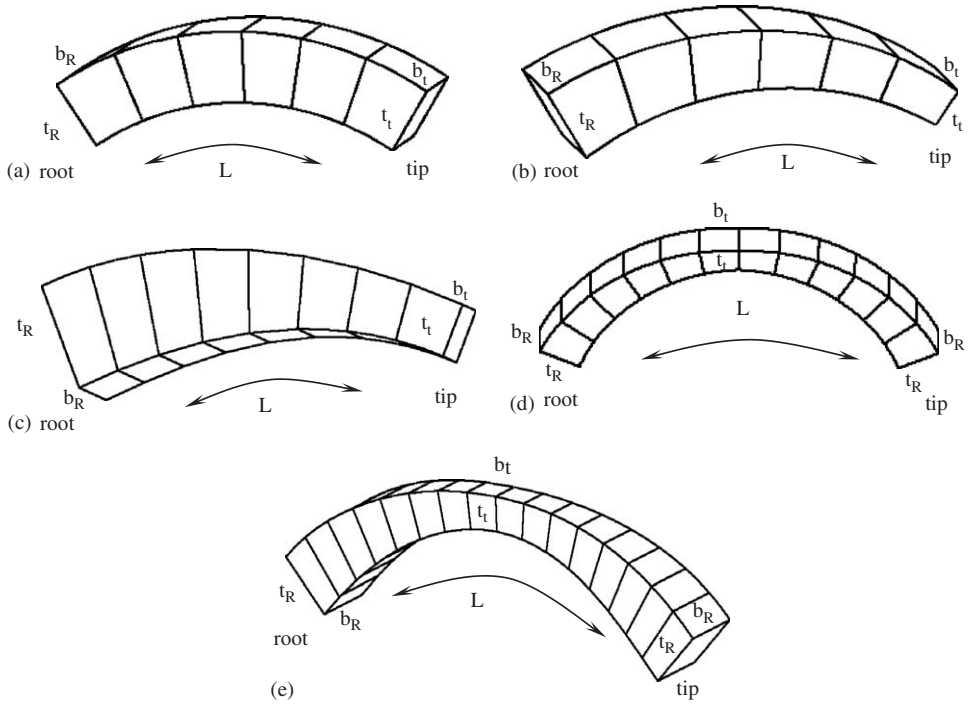

Fig. 2. Cross-sections of curved beams: (a) uniform ($C1$, $t_R = t_t$, $b_R = b_t$); (b) unsymmetric tapered with constant width ($C2$, $t_R \neq t_t$, $b_R = b_t$); (c) double unsymmetric tapered ($C3$, $t_R \neq t_t$, $b_R \neq b_t$); (d) symmetric tapered with constant width ($C4$, $t_R \neq t_t$, $b_R = b_t$); (e) double symmetric tapered ($C5$, $t_R \neq t_t$, $b_R \neq b_t$).

$C4$: Symmetric tapered with constant width ($t_R \neq t_t$, $b_R = b_t$, Fig. 2d),
$C5$: Double symmetric tapered ($t_R \neq t_t$, $b_R \neq b_t$, Fig. 2e),

$$t = \frac{(L - R\theta)}{L}(t_R - t_t) + t_t, \quad b = \frac{(L - R\theta)}{L}(b_R - b_t) + b_t. \tag{1}$$

The buckling and natural frequency parameters are represented by mathematical expressions to be used in numerical analysis as follows:

$$k_{\mathrm{cr}} = \sqrt{P_{\mathrm{cr}} R^3 / EI_{Root}}, \quad \lambda = \sqrt{\omega_1^2 \frac{\rho A_{Root} R^4}{EI_{Root}}}, \tag{2}$$

where

$$A_{Root} = t_R b_R, \quad I_{Root} = \frac{b_R t_R^3}{12}. \tag{3}$$

3. Theoretical analysis

The following two shape functions are used in the analysis to represent radial and circumferential deflections (Fig. 3), respectively [2],

$$w = a_1 \cos\phi + a_2 \sin\phi + a_4 - a_6\phi, \tag{4}$$

$$v = -a_1 \sin\phi + a_2 \cos\phi + a_3 + a_5\phi + a_6\phi^2/2. \tag{5}$$

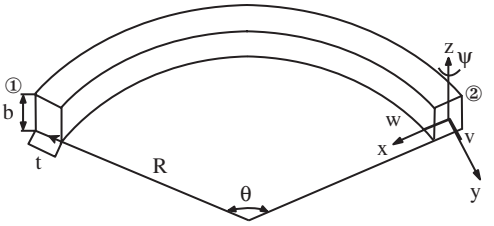

Fig. 3. Six degrees of freedom finite element model.

The deflection vector of the elemental finite element is

$$\mathbf{q}^{\mathrm{T}} = [v_1 w_1 \psi_1 v_2 w_2 \psi_2], \tag{6}$$

where

$$\psi = \frac{\mathrm{d}w}{\mathrm{d}y} - \frac{v}{R}. \tag{7}$$

The potential energy of the curved beam element is

$$U = \frac{1}{2}\left[\int_0^l EI_{xx}\left(w'' - \frac{v'}{R}\right)^2 + EA\left(\frac{w}{R} + v'\right)^2\right] dy. \tag{8}$$

Eq. (8) can be written in matrix form as

$$U = \tfrac{1}{2}\mathbf{q}^{\mathrm{T}}\mathbf{k}_e\mathbf{q} \tag{9}$$

The kinetic energy of the curved beam element is

$$T = \frac{1}{2}\int_0^l \rho A(\dot{w} + \dot{v})^2 \,\mathrm{d}y. \tag{10}$$

Eq. (10) can be written in matrix form as

$$T = \tfrac{1}{2}\dot{\mathbf{q}}^{\mathrm{T}}\mathbf{m}_e\dot{\mathbf{q}}. \tag{11}$$

The strain energy V denotes the work done by a uniformly distributed dynamic load $P(t)$ and given by the equation

$$V = \int_0^l P(t)R\left(\frac{\mathrm{d}w}{\mathrm{d}y} - \frac{v}{R}\right)^2 \mathrm{d}y. \tag{12}$$

Eq. (12) can be written in matrix form as

$$V = \tfrac{1}{2}\mathbf{q}^{\mathrm{T}}\mathbf{k}_g\mathbf{q}. \tag{13}$$

Thus, for a finite element, elastic stiffness matrix $\mathbf{k}_e$, element geometrical stiffness matrix $\mathbf{k}_g$ and mass matrix $\mathbf{m}_e$ are obtained, respectively.

Mass and stiffness matrices of each beam element are used to form global mass and stiffness matrices. The dynamic response of a beam for a conservative system can be formulated by means of Lagrange's equation of motion in which the external forces are expressed in terms of time-dependent potentials, and then performing the required operations the entire system leads to the governing matrix equation of motion

$$\mathbf{M}\ddot{\mathbf{q}} + \left[\mathbf{K}_e - P(t)\mathbf{K}_g\right]\mathbf{q} = 0. \tag{14}$$

The periodic uniformly distributed dynamic load $P(t) = P_o + P_t \cos \Omega t$ where Ω is the disturbing frequency, the static- and time-dependent components of the load can be represented as a fraction of the fundamental

static buckling load P_{cr} hence substituting $P(t) = \alpha P_{cr} + \beta P_{cr} \cos \Omega t$ in Eq. (14) it becomes

$$\mathbf{M}\ddot{\mathbf{q}} + \left[\mathbf{K}_e - \alpha P_{cr}\mathbf{K}_{gs} - \beta P_{cr} \cos(\Omega t)\mathbf{K}_{gt}\right]\mathbf{q} = 0, \tag{15}$$

where the matrices $\mathbf{K}_{gs}$ and $\mathbf{K}_{gt}$ in Eq. (15) reflect the influence of the static and time-dependent components of the load, respectively. Eq. (15) represents a system of second-order differential equation with periodic coefficients of the Mathieu–Hill type. From the theory of linear equations with periodic coefficients, the boundaries between stable and unstable solutions of Eq. (15) are formed by periodic solutions of period T and $2T$ where $T = 2\pi/\Omega$. It has been shown by Bolotin [1] that solutions with period $2T$ are the ones of greatest practical importance and that as a first approximation the boundaries of the principal regions of the dynamic instability can be determined from the equation:

$$\left[\mathbf{K}_e - \alpha P_{cr}\mathbf{K}_{gs} \pm \frac{1}{2}\beta P_{cr}\mathbf{K}_{gt} - \frac{\Omega^2}{4}\mathbf{M}\right]\mathbf{q} = 0. \tag{16}$$

The two matrices $\mathbf{K}_{gs}$ and $\mathbf{K}_{gt}$ will be identical if the static and time-dependent component of the loads are applied in the same manner. If $\mathbf{K}_{gs} \equiv \mathbf{K}_{gt} \equiv \mathbf{K}_g$ then Eq. (16) becomes

$$\left[\mathbf{K}_e - \left(\alpha \pm \frac{1}{2}\beta\right)P_{cr}\mathbf{K}_g - \frac{\Omega^2}{4}\mathbf{M}\right]\mathbf{q} = 0. \tag{17}$$

This equation represents the solution of the three related problems:

(i) Free vibration with $\alpha = 0$, $\beta = 0$, and $\omega = \Omega/2$ the natural frequency

$$[\mathbf{K}_e - \omega^2\mathbf{M}]\mathbf{q} = 0. \tag{18}$$

(ii) Static stability with $\alpha = 1$, $\beta = 0$ and $\Omega = 0$

$$[\mathbf{K}_e - P_{cr}\mathbf{K}_g]\mathbf{q} = 0. \tag{19}$$

(iii) Dynamic stability when all terms are present

$$\left[\mathbf{K}_e - \left(\alpha \pm \frac{1}{2}\beta\right)P_{cr}\mathbf{K}_g - \frac{\Omega^2}{4}\mathbf{M}\right]\mathbf{q} = 0. \tag{20}$$

4. Results and discussion

Two different finite element models, step and continuous, are developed to represent the variation of non-uniform cross-sections. The step model involves meshing a non-uniform cross-sectioned curved beam, consisting of a discrete number of elements each having a uniform cross-section. Whereas, the continuous model does not have uniform discrete elements, the variation of cross-section of the continuous model is represented by mathematical expressions given in Eq. (1).

Table 1 shows the results of the step and continuous finite element models for the critical buckling load and the fundamental frequency parameters for various numbers of elements. As seen from the table that even using as little as four elements both results are in close agreement. The results of Step model with 30 elements and Continuous model with 12 elements are almost identical. Computing time for the Step model with 30 elements is less than 1 s and for the Continuous model with 12 elements is 45 s. The Continuous model converges faster and represents the variation of cross-section better than the step model. Since the integration is carried out one by one to form mass, elastic stiffness and geometric stiffness matrices of each element, computing time takes longer for the Continuous Model. In order to save computing time as well as not being able to show the difference of the results obtained by using the developed finite element models in graphical forms, only the results of step model are used in the graphical representations.

The exact solution of analytical static stability formulation (critical buckling load parameter) for a uniform fixed–fixed curved beam is given by Timoshenko [18]. Table 2 gives the comparison of the exact solution of

Table 1
Comparison of the critical buckling load and fundamental frequency parameters between the step (A and I_{xx}) and continuous ($A(y)$ and $I_{xx}(y)$) finite element models, $b_t/b_R = 0.5$, $t_t/t_R = 0.5$ ($C3$)

Number of elements	k_{cr} ratio critical buckling load parameters		λ ratio fundamental frequency parameters	
	Finite element model: step (A and I_{xx})	Finite element model: continuous ($A(y)$ and $I_{xx}(y)$)	Finite element model: step (A and I_{xx})	Finite element model: continuous ($A(y)$ and $I_{xx}(y)$)
2	6.392	6.183	57.225	55.621
4	4.267	4.365	39.432	40.088
6	4.334	4.265	39.369	39.292
8	4.293	4.257	39.276	39.150
10	4.273	4.252	39.223	39.110
12	4.264	4.250	39.192	39.095
30	4.251	4.248	39.127	39.082

$b_R = 20\,\text{mm}$, $t_R = 4\,\text{mm}$, $\theta = 60^\circ$, $R = 250\,\text{mm}$, $E = 6.89 \times 10^{10}\,\text{N/m}^2$, $\rho = 2770\,\text{kg/m}^3$.

Table 2
Convergence characteristics of critical buckling load parameters of the present FEM model with the number of elements, for a uniform cross-section curved beam, $\theta = 60^\circ$, k_{exact}: 8.621, $R = 762\,\text{mm}$, $b = 25.4\,\text{mm}$, $t = 2\,\text{mm}$, $E = 6.89 \times 10^{10}\,\text{N/m}^2$, $\rho = 2770\,\text{kg/m}^3$

Number of elements	k_{cr} ratio critical buckling load parameter k_{exact}: 8.621	
	Step model	Continuous model
2	10.5304	10.526
4	8.7729	8.769
6	8.6849	8.681
8	8.6666	8.663
10	8.6612	8.658
12	8.6593	8.656
30	8.6574	8.654

parametric critical buckling load with the solution of present finite element models for various numbers of elements of a uniform fixed–fixed curved beam. As seen from the table, agreement between the present finite element models and exact solution results is very good.

The exact solution and the finite element solutions of the fundamental frequency for a uniform fixed–fixed curved beam are given by Refs. [3,7,8]. Table 3 gives the comparison of the fundamental frequency obtained by the present finite element models and finite element solutions of other investigators for a uniform fixed–fixed curved beam. Pety and Fleischer [3] used three different displacement functions in their analysis and show the accuracy of the functions by comparing the results. Two different displacement functions with internal nodes were used by Sabuncu [7] for the vibration analysis of uniform curved beams. Sabuncu and Erim [8] investigated the vibration analysis of uniform and non-uniform cross-sectioned curved beams. As seen from the table, the results of uniform finite element models based on simple strain functions with or without internal nodes are in close agreement.

Table 4 shows comparison of the fundamental frequency parameter (λ) between the present models and results of Ref. [17] for symmetric tapered curved beam with constant width ($C4$) having fixed–fixed boundary conditions. Close agreement is found.

Effect of opening angle of curvature on the critical buckling load is shown in Fig. 4. When the opening angle of an arch increases, it means the length of the arch increases, and as a result the curved beam becomes more flexible. Thus, as shown in Fig. 4, the critical buckling load decreases. It can be noticed from the figure that

Table 3
Comparison of the fundamental frequency between the present model ($C1$) and the other investigators FEM results for various number of elements and frequencies, $A = 8.387\,\text{mm}^2$, $L = 101.6\,\text{mm}$, $R = 762\,\text{mm}$, $t^2/12R^2 = 0.154 \times 10^{-7}$, $E = 6.89 \times 10^{10}\,\text{N/m}^2$, $\rho = 2770\,\text{kg/m}^3$

Mode		Frequency (Hz)														
		Pety and Fleischer [3]			Sabuncu [7]			Sabuncu and Erim [8]			Present results					
	[a]	4	6	8	2	3	4	4	6	8	4		6		8	
	[b]										Step	Cont	Step	Cont	Step	Cont
1	1	667	557	513	423	423	423	456	452	452	455	452	453	449	452	448
	2	597	504	469	448	448	448									
	3	453	449	448												
2	1	857	791	760	688	686	686	732	719	717	732	728	719	716	716	713
	2	803	759	732	714	712	712									
	3	730	716	713												
3	1	1301	1152	1120	1069	1057	1057	1038	1087	1086	1088	1084	1088	1085	1086	1082
	2	1201	1144	1104	1094	1081	1081									
	3	1007	1085	1082												
4	1	1791	1611	1537	1394	1377	1373	1712	1491	1474	1711	1698	1490	1478	1473	1462
	2	2660	1617	1523	1483	1458	1454									
	3	1703	1480	1463												
5	1	2945	2400	2292	2226	2103	2073	2839	2255	2234	2840	2818	2249	2232	2232	2215
	2	3973	2366	2299	2369	2224	2192									
	3	2838	2235	2216												
6	1	4633	3495	3182	4980	2903	2881	4552	3480	3123	4562	4526	3472	3445	3124	3100
	2	6065	3915	3205	5292	3076	3050									
	3	4584	3448	3102												

[a]Number of elements.
[b]Different displacement functions used.

Table 4
Comparison of the fundamental frequency parameter (λ) between the present model and Ref. [17] results for symmetric tapered with constant width ($C4$), $R = 750\,\text{mm}$, $t_t = 3\,\text{mm}$, $b = 20\,\text{mm}$, $E = 6.89 \times 10^{10}\,\text{N/m}^2$, $\rho = 2770\,\text{kg/m}^3$

	$t_t/t_R = 0.9$			$t_t/t_R = 0.83$			$t_t/t_R = 0.77$		
θ°	Present		[17]	Present		[17]	Present		[17]
	Step	Cont.		Step	Cont.		Step	Cont.	
20	535.4176	534.9801	535.4500	566.6669	566.2039	566.8193	597.4190	596.9309	597.7229
30	236.5006	236.3074	236.5183	250.3578	250.1533	250.3404	263.9959	263.7802	264.1372
40	131.8963	131.7886	131.9088	139.6661	139.5520	139.7107	147.3139	147.1936	147.3984
50	83.4974	83.4292	83.5073	88.4493	88.3771	88.4809	93.3243	93.2481	93.3824

Step model: 30 elements.Continuous model: 12 elements.

critical buckling load values of beams having $C2$ and $C4$ type cross-sections are close to each other. There is a similar phenomenon between $C3$ and $C5$ type cross-sectioned curved beams. Critical buckling loads of single tapered curved beams ($C2$ and $C4$) are higher than the double tapered curved beams ($C3$ and $C5$), respectively, as expected. It can also be noticed that even though the thickness of $C4$ tapers twice as much as $C2$ and the thickness and width of $C5$ tapers twice as much as $C3$ type beams. It seems that symmetric tapered beams are more stable than expected.

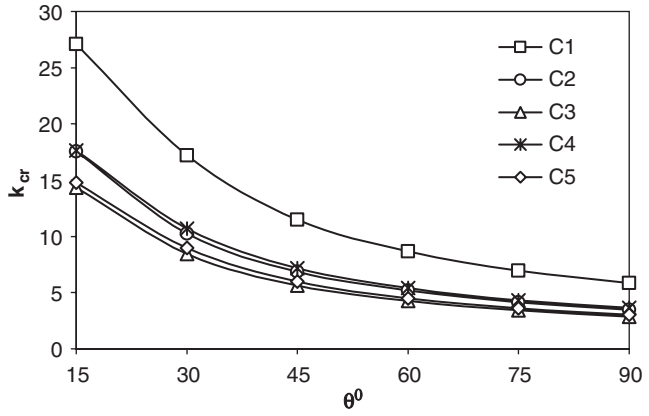

Fig. 4. Effect of variation of opening angle of an arch on the critical buckling load parameter for various cross-sections. $b_t/b_R = t_t/t_R = 1$ (□ $C1$), $b_t/b_R = 1$ and $t_t/t_R = 0.5$ (○ $C2$ and ✱ $C4$), $b_t/b_R = t_t/t_R = 0.5$ (△ $C3$ and ◇ $C5$).

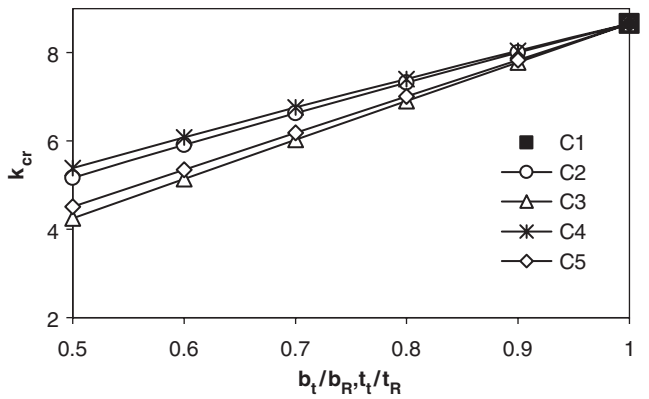

Fig. 5. Effect of thickness variation of a curved beam on the critical buckling load parameter for various cross-sections. $\theta = 60^\circ$, $b_t = b_R$, $t_t = t_R$ (■ $C1$), $b_t = b_R$, $t_R \neq t_t$ (○ $C2$ and ✱ $C4$), $b_t \neq b_R$, $t_t \neq t_R$ (△ $C3$ and ◇ $C5$).

In Fig. 5, it is seen that when the variation of cross-section diminishes and approaches the uniform cross-section, the curved beam becomes stiffer; as a result, the critical buckling load increases and takes the value of the uniform cross-sectioned curved beam. From this figure, it can be said that static stability values of curved beams having $C3$, $C5$, $C2$ and $C4$ type cross-sections increases, respectively. This increase decreases as the cross-section variation diminishes.

It can be noticed from Fig. 6 that when the opening angle of an arch increases, the fundamental frequency parameter decreases for all the cross-sections as expected. It can also be noticed that the frequency parameters of $C4$ and $C1$ cross-sectioned curved beams are fairly close at about $\theta = 25^\circ$. Beyond this angle (30°–90°), the fundamental frequency parameter of $C5$ cross-sectioned curved beam is higher than the fundamental frequencies of other type cross-sectioned curved beams. This is due to shape factor. In addition, the frequency parameters of $C3$ and $C2$ are almost identical.

When the opening angle of an arch increases, the fundamental frequency parameters of curved beams having the same length but five different cross-sections come closer. This phenomenon can be explained as follows: when the opening angle of an arch increases, the length of curved beams also increases, consequently beams become very flexible. The length variation effect on the flexibility is more dominant than the effect of variation of cross-section.

As shown in Fig. 7, if the variation of the cross-section diminishes and approaches the uniform cross-section, the fundamental frequency parameters of $C2$, $C3$ and $C4$ cross-sectioned curved beams increase and

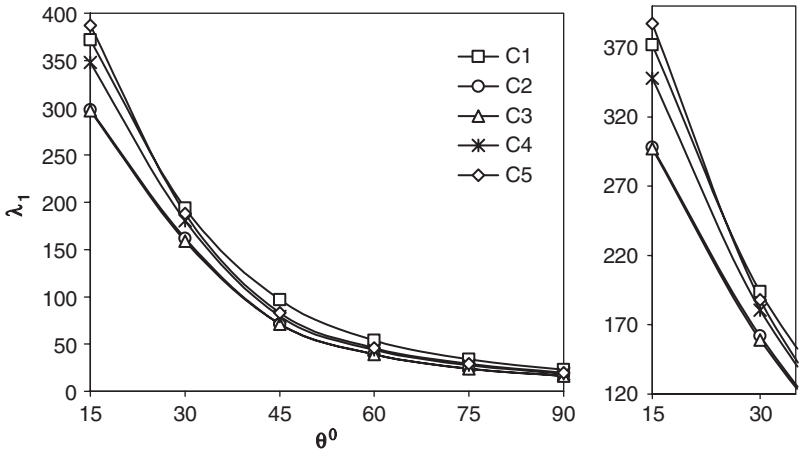

Fig. 6. Effect of variation of opening angle of an arch on the fundamental frequency parameter for various cross-sections. $b_t/b_R = t_t/t_R = 1$ (□ $C1$), $b_t/b_R = 1$ and $t_t/t_R = 0.5$ (○ $C2$ and ✱ $C4$), $b_t/b_R = t_t/t_R = 0.5$ (△ $C3$ and ◇ $C5$).

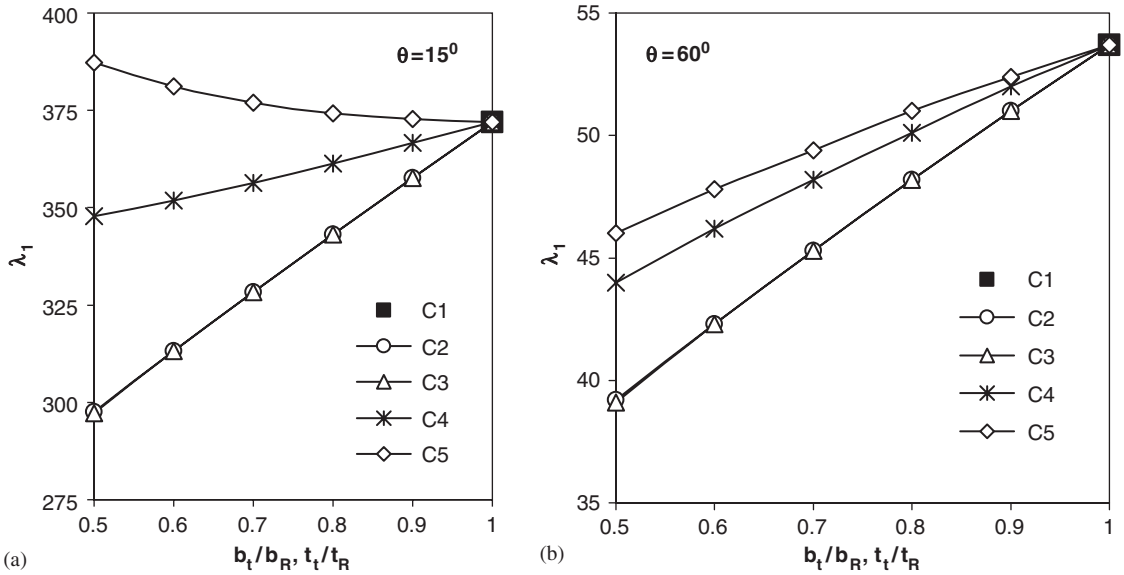

Fig. 7. Effect of thickness variation of a curved beam on the fundamental frequency parameters for various cross-sections. (a) $\theta = 15^\circ$; (b) $\theta = 60^\circ$, $b_t = b_R$, $t_t = t_R$ (■ $C1$), $b_t = b_R$, $t_R \neq t_t$ (○ $C2$ and ✱ $C4$), $b_t \neq b_R$, $t_t \neq t_R$ (△ $C3$ and ◇ $C5$).

approach the frequency parameter of $C1$ cross-sectioned curved beam. On the other hand, the fundamental frequency parameter of $C5$ cross-sectioned curved beam decreases and approaches the fundamental frequency of the $C1$ cross-sectioned curved beam for $\theta = 15^\circ$, while it increases and approaches the frequency parameter of $C1$ cross-sectioned curved beam for $\theta = 60^\circ$.

From Fig. 8(a), it can be noticed that the first dynamic instability region widens because of the increase in the opening angle of the arch. Although the cross-sectional area of $C1$ cross-sectioned curved beam is larger than the other cross-sections, $C1$ cross-sectioned curved beam is less stable compared to other cross-sections. The reason for this is that as in the case of the fundamental frequency, the mass and elastic stiffness as well as symmetric features of curved beams are quite influential on the dynamic stability. In addition, when the dynamic load parameter increases, the unstable region widens. As shown in Fig. 8(b), the second dynamic

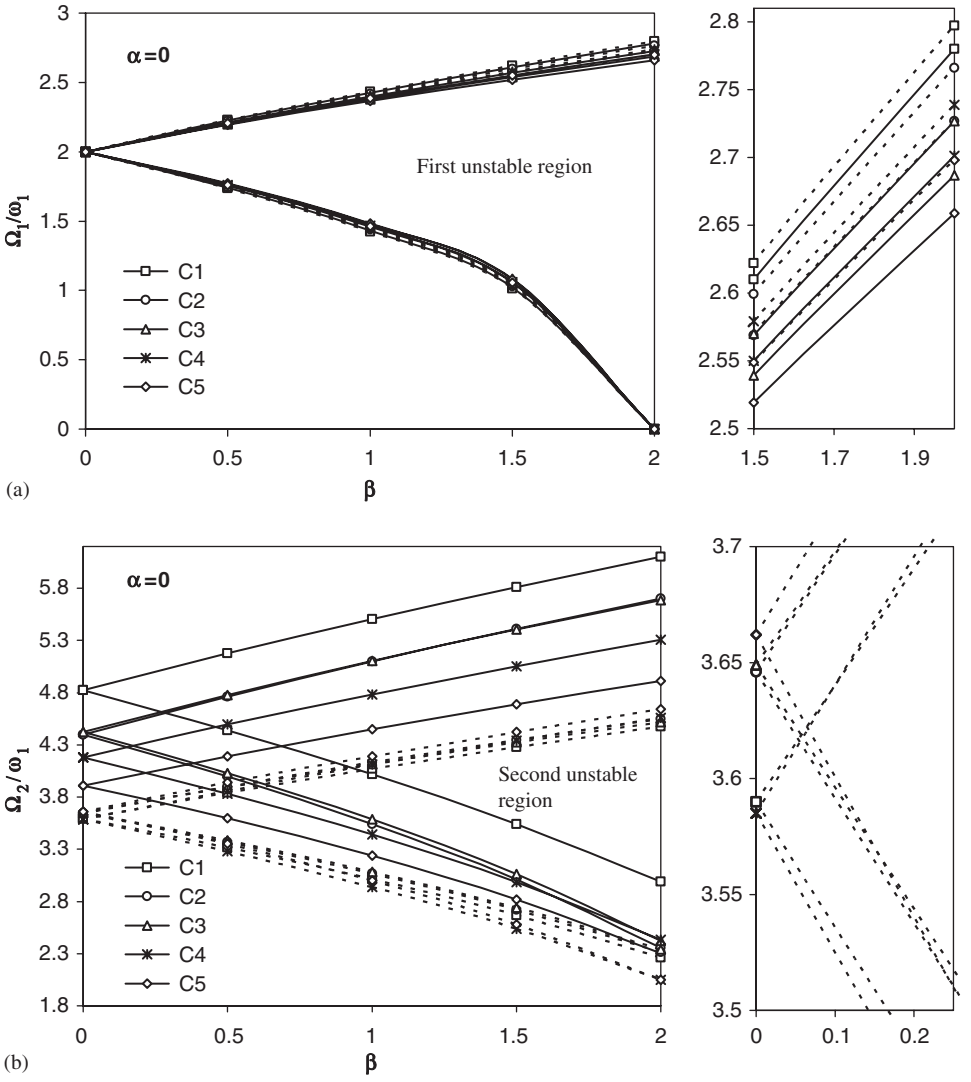

Fig. 8. The effect of dynamic load parameter on the first and second dynamic stabilities regions of curved beams for various cross-sections and two different opening angles. (a) First unstable region. (b) Second unstable region. $\alpha = 0$, $b_t/b_R = t_t/t_R = 1$ (□ $C1$), $b_t/b_R = 1$ and $t_t/t_R = 0.5$ (○ $C2$ and ✱ $C4$), $b_t/b_R = t_t/t_R = 0.5$ (△ $C3$ and ◇ $C5$). ..... $\theta = 60^\circ$, ___ $\theta = 15^\circ$.

instability regions move towards origin and are close to each other, when the opening angle of the arch increases. From the figure, it can be noticed that the location of the second stability region is scattered and sequences of these stability regions move down as $C1$, $C3$, $C2$, $C4$ and $C5$ at $\theta = 15^\circ$ and $C5$, C3, $C2$, $C1$ and $C4$ at $\theta = 60^\circ$.

As shown in Figs. 9(a) and (b), if the static load parameter increases, the initial ratio of the disturbing frequency to the fundamental frequency scatters and moves towards origin. It can be seen from the figures that the curved beam under periodic loading becomes unstable at a small disturbing frequency and small dynamic load parameter. When the static load parameter is equal to 0.25, the upper borders of the first unstable region of the all-curved beams intersect at $\Omega_1/\omega_1 = 2$ for $\beta = 0.5$. In addition, for $\theta = 60^\circ$ the sequence of second stability region is different from Fig. 8b.

Figs. 10(a) and 11(a) shows that when b_t/b_R and t_t/t_R ratios approach unity for $\alpha = 0$ and $\alpha = 0.25$, the first unstable region approaches the region of $C1$ cross-sectioned curved beam. For both figures, the order of the first stability regions of all cross-sections does not change from the stability point of view.

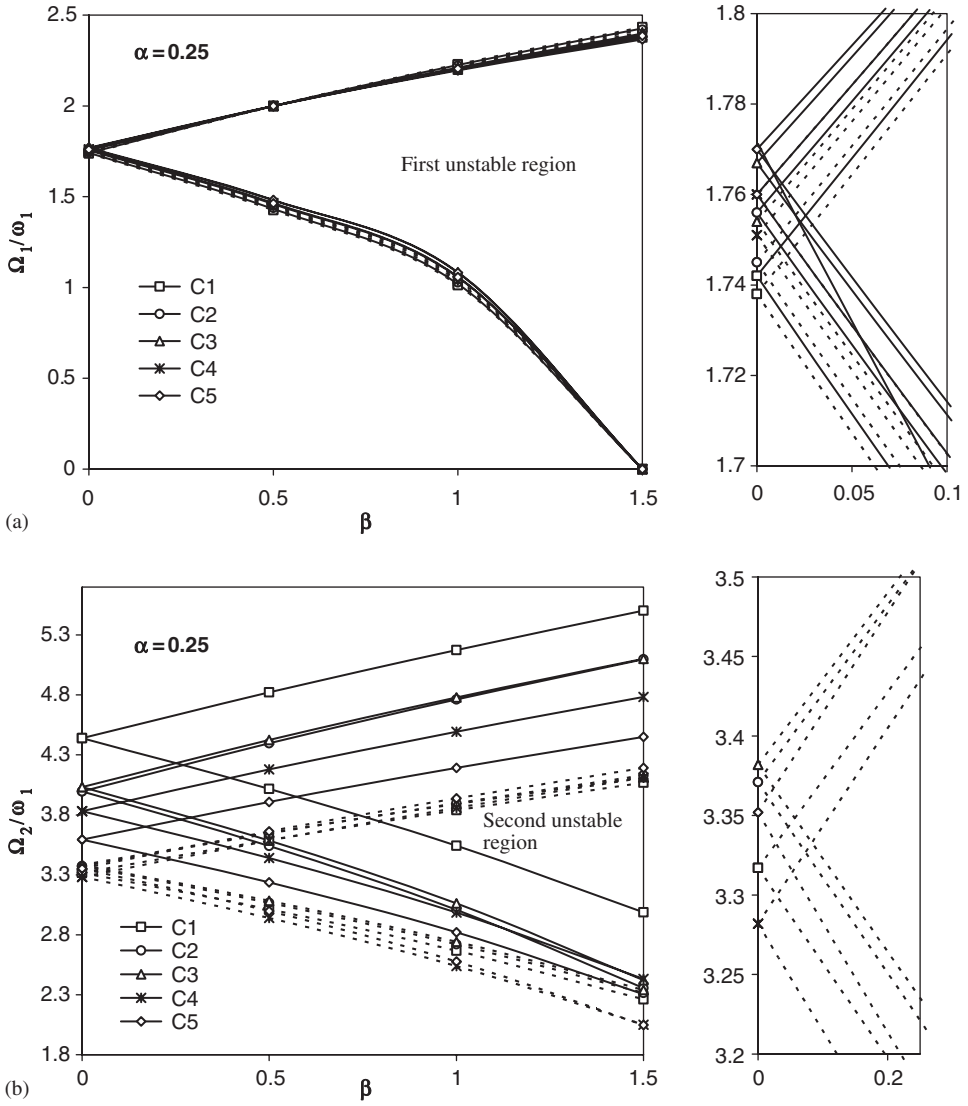

Fig. 9. The effect of dynamic load parameter on the first and second dynamic stabilities regions of curved beams for various cross-sections and two different opening angles. (a) First unstable region. (b) Second unstable region. $\alpha = 0.25$, $b_t/b_R = t_t/t_R = 1$ (□ $C1$), $b_t/b_R = 1$ and $t_t/t_R = 0.5$ (○ $C2$ and ✱ $C4$), $b_t/b_R = t_t/t_R = 0.5$ (△ $C3$ and ◇ $C5$). ..... $\theta = 60°$, ___ $\theta = 15°$.

When b_t/b_R and t_t/t_R ratios approach unity, the second unstable region approaches the region of $C1$ cross-sectioned curved beam as expected in Figs. 10(b) and 11(b). However, it can be observed in these figures that the orders of the second stability regions for $C1$, $C2$, $C3$, $C4$ and $C5$ change for $\alpha = 0$ and $\alpha = 0.25$ conditions.

5. Conclusions

In this paper, the dynamic and static stability of non-uniform cross-sectioned curved beams are studied and the following conclusions are drawn:

- When the opening angle of an arch increases, the static stability decreases and the first dynamic instability region widens. On the other hand, the second instability regions shift to the origin.

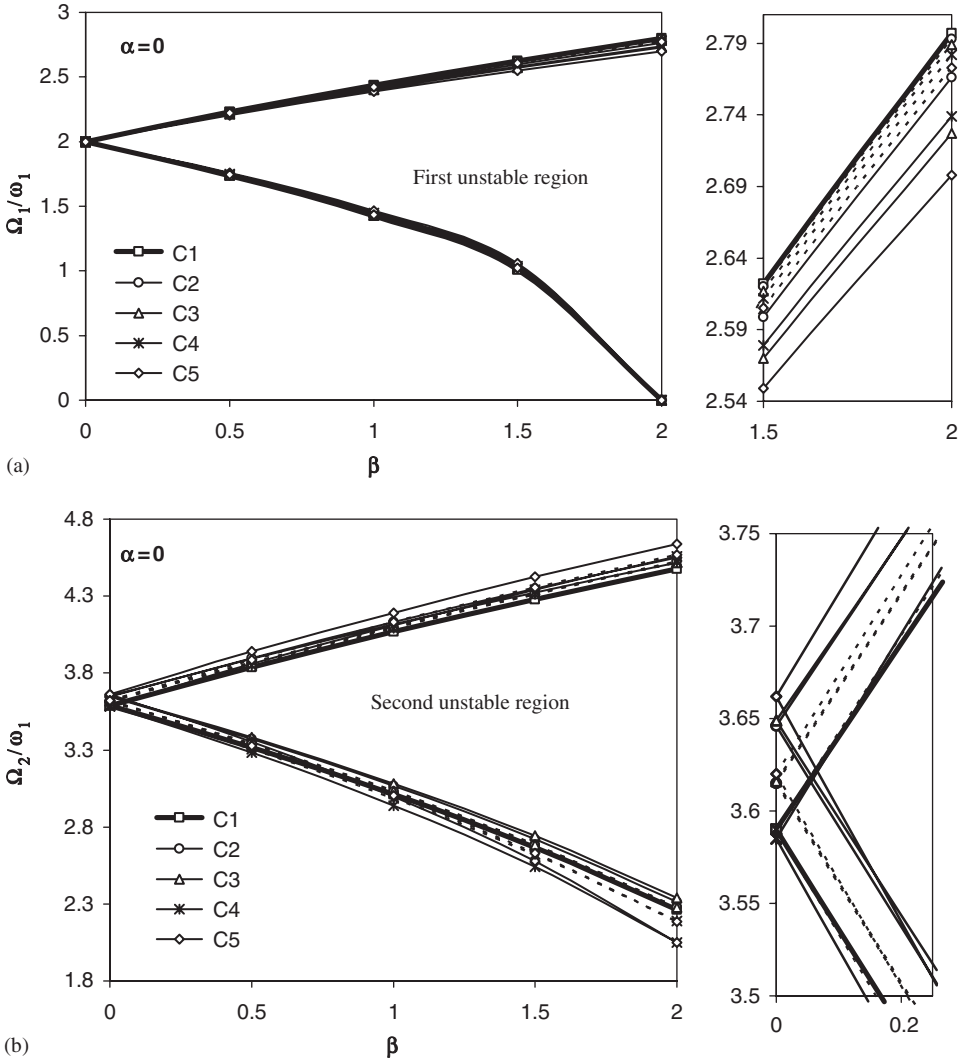

Fig. 10. The effect of dynamic load parameter on the dynamic stability regions of curved beams for various cross-sections of a curved beam. (a) First unstable region. (b) Second unstable region. $\alpha = 0$, $\theta = 60^\circ$, $b_t = b_R$, $t_t = t_R$ ($C1$), $b_t = b_R$, $t_R \neq t_t$ ($C2$ and $C4$), $b_t \neq b_R$, $t_t \neq t_R$ ($C3$ and $C5$). ___ $b_t/b_R = t_t/t_R = 0.5$ (△ $C3$ and ◇ $C5$), ___ $b_t/b_R = 1$, $t_t/t_R = 0.5$ (○ $C2$ and ✱ $C4$), ... $b_t/b_R = t_t/t_R = 0.8$ (△ $C3$ and ◇ $C5$), ... $b_t/b_R = 1$, $t_t/t_R = 0.8$ (○ $C2$ and ✱ $C4$), ▬ $b_t/b_R = t_t/t_R = 1$ (□ $C1$).

- When the cross-section of a non-uniform curved beam approaches uniform cross-section, the curved beam becomes more stable from the static stability point of view.
- If the static load parameter is equal to 0.25, the initial ratios of the first and second disturbing frequency to the fundamental frequency scatter and move towards origin. The dynamic load parameter is bounded between the values of zero and 1.5 for the first dynamics instability regions.
- For $\theta = 60^\circ$, the sequences of the second dynamic instability regions for $\alpha = 0.25$ condition are different than $\alpha = 0$ condition.
- The unstable region is affected by the variation of cross-section of a curved beam. As indicated in Figs. 10 and 11, the first unstable region of uniform cross-sectioned curved beams is wider and closer to origin than the other non-uniform cross-sectioned curved beams. But this phenomenon is not valid for the second unstable regions. The second unstable region of $C4$ cross-sectioned curved beam is closer to origin than the other cross-sectioned curved beam.

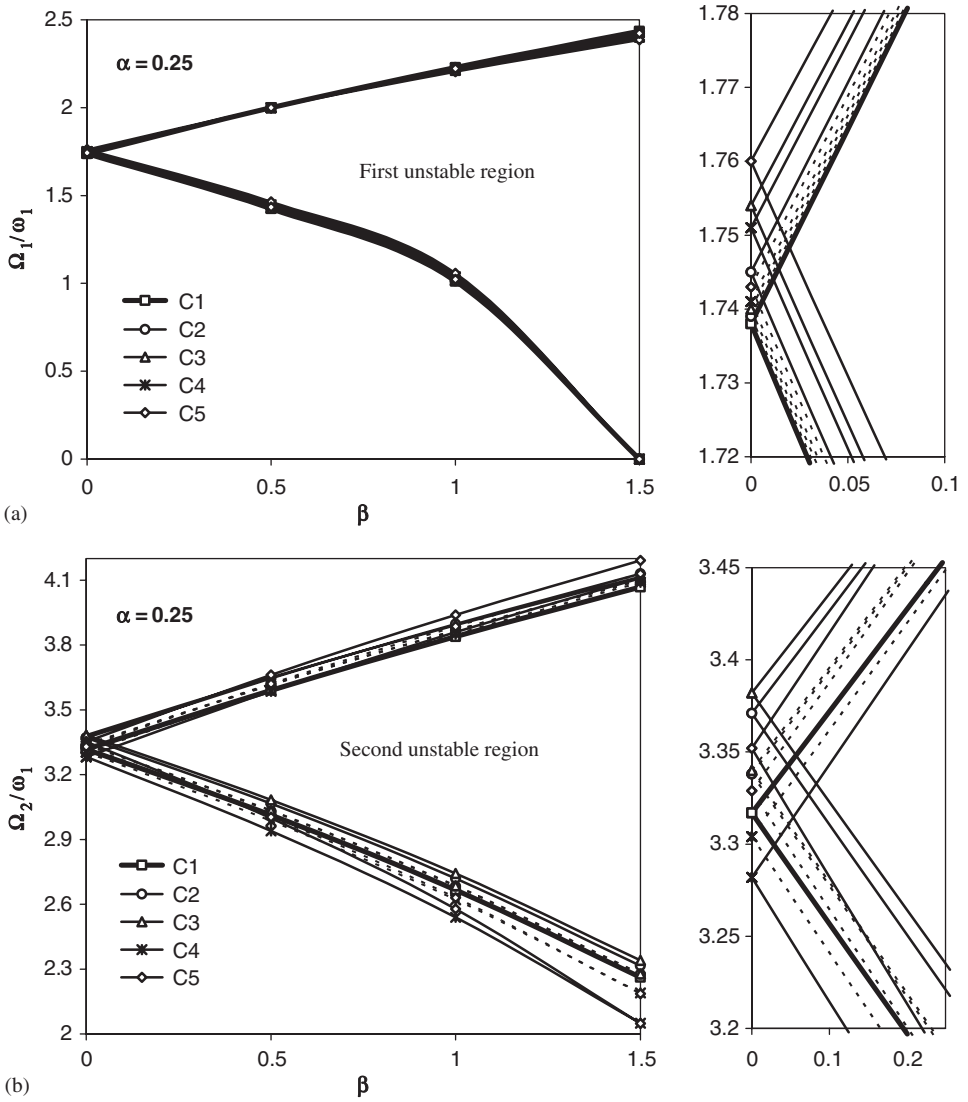

Fig. 11. The effect of dynamic load parameter on the dynamic stability regions of curved beams for various cross-sections of a curved beam. (a) First unstable region. (b) Second unstable region: $\alpha = 0.25$, $\theta = 60^{\circ}$, $b_t = b_R$, $t_t = t_R$ ($C1$), $b_t = b_R$, $t_R \neq t_t$ ($C2$ and $C4$), $b_t \neq b_R$, $t_t \neq t_R$ ($C3$ and $C5$). ___ $b_t/b_R = t_t/t_R = 0.5$ (△ $C3$ and ◇ $C5$), ___ $b_t/b_R = 1$, $t_t/t_R = 0.5$ (○ $C2$ and ✱ $C4$), ... $b_t/b_R = t_t/t_R = 0.8$ (△ $C3$ and ◇ $C5$), ... $b_t/b_R = 1$, $t_t/t_R = 0.8$ (○ $C2$ and ✱ $C4$), ▬ $b_t/b_R = t_t/t_R = 1$ (□ $C1$).

Finally, by changing the static and dynamic load parameters, type of the cross-section of a curved beam, the ratios of dimensions of thickness and width at the tip cross-section to the ones at the root cross-section of the curved beam, the dynamic stability of the curved beam may be conserved.

References

[1] V.V. Bolotin, *Dynamic Stability of Elastic Systems*, Holden Day, San Francisco, 1964.
[2] A.B. Sabir, D.G. Ashwell, A comparison of curved beam finite elements when used in vibration problem, *Journal of Sound and Vibration* 18 (4) (1971) 555–563.
[3] M. Petyt, C.C. Fleischer, Free vibration of a curved beam, *Journal of Sound and Vibration* 18 (1) (1971) 17–30.
[4] V. Yıldırım, A computer program for the free vibration analysis of elastic arcs, *Computer & Structures* 62 (3) (1997) 475–485.

[5] S.S. Rao, Effects of transverse shear and rotary inertia on the coupled twist-bending vibrations of circular rings, *Journal of Sound and Vibration* 16 (4) (1971) 551–566.
[6] E. Moshe, E. Efraim, In-plane vibration of shear deformable curved beams, *International Journal for Numerical Methods in Engineering* 52 (2001) 1221–1234.
[7] M. Sabuncu, Vibration Characteristics of Rotating Aerofoil Cross-section Bladed-disc Assembly, PhD Thesis, University of Surrey, 1978.
[8] M. Sabuncu, S. Erim, In-plane vibration of a tapered curved beam, *Proceeding of the Seventh World Congress on the Theory of Machines an Mechanisms*, Sevilla, Spain, 1987.
[9] P. Chidamparam, A.W. Leissa, Vibration of planar curved beams, rings, and arches, *Applied Mechanical Reviews* 46 (9) (1993) 467–483.
[10] P. Chidamparam, A.W. Leissa, Influence of centerline extensibility on the in-plane free vibration of loaded circular arches, *Journal of Sound and Vibration* 183 (5) (1995) 779–795.
[11] R.E. Rossi, P.A.A. Laura, P.L. Verniere De Irassar, In-plane vibrations of cantilevered non-circular arcs of non-uniform cross-section with a tip mass, *Journal of Sound and Vibration* 129 (2) (1989) 201–213.
[12] R.H. Gutierrez, P.A.A. Laura, R.E. Rossi, R. Bertero, A. Villaggi, In-plane vibrations of non-circular arcs of non-uniform cross-section, *Journal of Sound and Vibration* 129 (2) (1989) 181–200.
[13] R.E. Rossi, In-plane vibrations of circular rings of non-uniform cross-section with account taken of shear and rotatory inertia effects, *Journal of Sound and Vibration* 135 (3) (1989) 443–452.
[14] X. Tong, N. Mrad, B. Tabarrok, In-plane vibration of circular arches with variable cross-sections, *Journal of Sound and Vibration* 212 (1) (1998) 121–140.
[15] S.J. Oh, B.K. Lee, I.W. Lee, Free vibration of non-circular arches with non-uniform cross-section, *International Journal of Solids and Structures* 37 (2003) 4871–4891.
[16] M. Kawakami, T. Sakiyama, H. Matsuda, C. Morita, In-plane and out-of-plane free vibrations of curved beams with variable sections, *Journal of Sound and Vibration* 187 (3) (1995) 381–401.
[17] G. Karami, P. Malekzadeh, In-plane free vibration analysis of circular arches with varying cross-sections using differential quadrature method, *Journal of Sound and Vibration* 274 (3–5) (2004) 777–799.
[18] S.P. Timoshenko, J.M. Gere, *Theory of Elastic Systems*, McGraw-Hill Book Company, New York, 1961.
[19] Z.P. Bazant, L. Cedolin L, *Stability of Structures*, Oxford University Press, New York, 1991.
[20] H.C. Yoo, Y.J. Kang, J.S. Davidson, Buckling analysis of curved beams by finite-element discretization, *Journal of Engineering Mechanics* 122 (1996) 762–770.
[21] J.P. Papangelis, N.S. Trahair, In-plane finite element analysis of arches, School of Civil and Mining Engineering, The University of Sydney, Research Report No. R523, 1986.
[22] J.P. Papangelis, N.S. Trahair, Finite element analysis of arch lateral buckling, School of Civil and Mining Engineering, The University of Sydney, Research Report No. R524, 1986.
[23] Y.B. Yang, S.R. Kuo, Effect of curvature on stability of curved beams, *Journal of structural Engineering* 113 (6) (1987) 1185–1202.
[24] Y.B. Yang, S.R. Kuo, J.D. Yau, Use of straight-beam approach to study buckling of curved beams, *Journal of structural Engineering* 117 (7) (1991) 1963–1977.
[25] H. Matsunaga, In-plane vibration and stability of shallow circular arches subjected to axial forces, *International Journal of Solids and Structures* 33 (4) (1996) 469–482.
[26] K.J. Kang, C.W. Bert, A.G. Striz, Vibration and buckling analysis of circular arches using DQM, *Computer & Structures* 60 (1) (1996) 49–57.
[27] Y.L. Pi, M.A. Bradford, B. Uy, In-plane stability of arches, *International Journal of Solids and Structures* 39 (2002) 105–125.
[28] C.S. Huang, K.Y. Nieh, M.C. Yang, In-plane free vibration and stability of loaded and shear-deformable circular arches, *International Journal of Solids and Structures* 40 (2003) 5865–5886.
[29] L.W. Chen, G.S. Shen, Vibration and buckling of initially stressed curved beams, *Journal of Sound and Vibration* 215 (3) (1998) 511–526.
[30] J. Thomas, B.A.H. Abbas, Dynamic stability of Timoshenko beam by finite element method, *Journal of Engineering for Industry, Transaction of ASME* 98 (1976) 1145–1151.
[31] K. Takahashi, Y. Natsuaki, Y. Konishi, Dynamic stability of a circular arch subjected to distributed in-plane dynamic force, *Journal of Sound and Vibration* 146 (2) (1991) 211–221.
[32] L. Briseghella, C.E. Majorana, C. Pellegrino, Dynamic stability of elastic structures: a finite element approach, *Computer & Structures* 69 (1998) 11–25.
[33] N.I. Kim, K.J. Seo, M.Y. Kim, Free vibration and spatial stability of non-symmetric thin-walled curved beams with variable curvatures, *International Journal of Solids and Structures* 40 (2003) 3107–3128.